

A novel technological process for fabricating micro-tips for biomimetic adhesion

G La Spina, C Stefanini, A Menciassi and P Dario

Scuola Superiore Sant'Anna, CRIM Lab, Polo Sant'Anna Valdera, Viale Rinaldo Piaggio 34, 56025, Pontedera (Pisa), Italy

E-mail: giannilas pina@crim.sssup.it, cesare@sss up.it, arianna@sss up.it and dario@sss up.it

Received 25 March 2005, in final form 24 May 2005

Published 28 June 2005

Online at stacks.iop.org/JMM/15/1576

Abstract

In this paper, the issue of adhesion to biological substrates for biomedical applications is addressed. In particular, taking inspiration from intestinal parasites, micro-hooks for clamping on the gastrointestinal wall have been studied, in order to provide future endoscopic micro-systems with the capability of attaching safely to the mucosa surface. A novel fabrication technology and experimentation on nylon micro-hooks are presented, together with theoretical modelling of the process. Artificial hooks have been prototyped (length ranging between 300 μm and 500 μm ; maximum diameter of 100 μm) and a batch process for large array production has been proposed.

1. Introduction

Adhesion is an important issue in biomedical problems, where minimally invasive artificial systems have to be developed for human body exploration and monitoring. The medical purpose is to move and operate directly inside the human body, in particular in the gastrointestinal tract. The final target of these studies is to perform endoscopic screening for an early detection of cancer (at present early detection is the most powerful tool to overcome such disease) [1]. To achieve such goals a system to efficiently and safely adhere to biological tissues is required.

Gastrointestinal wall is irregular, slippery, chemically corrosive and physiologically active due to peristalsis. No traditional technologies enable an effective clamping on such a surface for prolonged time and without provoking damage or bleeding.

On the other hand, nature has conceived a wide variety of strategies to perform adhesion in the most difficult situations: hooking, snapping, suction, gluing and friction are some of these strategies (figure 1) [2]. Biomechanics of plants and animals can be very helpful to develop artificial structures and machines able to stop at a fixed point of the gastrointestinal tract or to produce a lever effect for locomotion [3].

Research studies are now trying to understand the basic principles regulating some effective adhesion systems

exploited in biological creatures, to simulate those systems and to replicate their mechanisms [4]. In particular *Taenia Solium* (tapeworm), the well-known parasite of the human gut, has some peculiar features to enhance its ability to adhere onto biological tissues: its adhesion system exploits four suckers and a set of micro-hooks, allowing the parasite to fix to the duodenum wall without damaging the intestinal surface, thanks to their small dimensions. Therefore, hooking represents an effective strategy for adhesion to this kind of biological tissue.

The aim of this work is to model and fabricate biomimetic hooks to be exploited for artificial adhesion to biological tissues: this issue involves many dimensional constraints (typical sizes of the order of 100 μm), shaping problems (sharp tips and 3D geometries) and material issues. The problem of adhesion is faced according to a biomimetic approach; once the optimal hook shape is identified, a novel micro-fabrication technology is purposely developed and illustrated.

The proposed approach consists of an innovative method: a drop of melted polymer is deposited between two heated moving substrates. Thus, a sort of liquid bridge occurs thanks to capillarity effects. Substrates are then moved far from each other, with controlled stroke and speed.

A numerical simulation of the 'liquid bridge process' has been made in order to achieve a well-controlled and repeatable method. Mathematical modelling and simulation

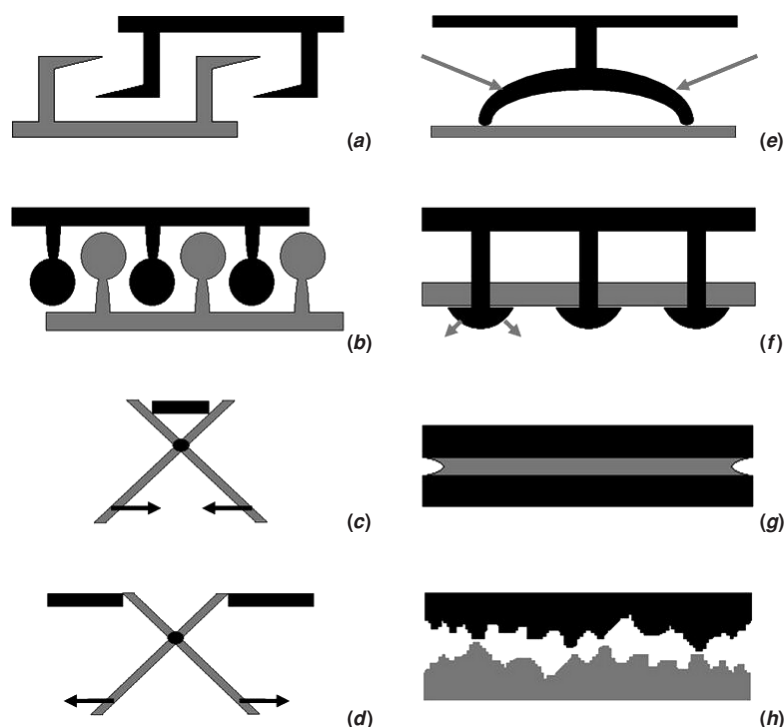


Figure 1. Eight fundamental locking systems exploited in biology: (a) hook, (b) snap, (c) claw, (d) lever, (e) sucker, (f) expansion anchorage, (g) adhesive secretion (glue), (h) friction.

of the ‘liquid bridge’ is followed by the experimental setup and tests.

Finally, a batch process is proposed for the fabrication of multiple hooks, integrated in a biomimetic membrane for future hook activation.

2. Bio-inspiration

The importance of a biomimetic approach for problems such as the safe adhesion to biological tissues mainly lies in the following aspects:

- biomedical micro-machines are still at an early stage of development, where no wide experience and technologies are available. Thus nature solutions can be considered as valid models for inspiration [5];
- the only way to achieve an acceptable miniaturization is to integrate different functions into the same device; the biological world is a perfect example of high and effective integration;
- in the case of autonomous devices, energetic issues require high efficiency, that is a peculiar feature of living systems.

Whereas looking at nature’s solutions, animals solved the problem of adhesion to unstructured substrates in different ways. Some fish of the mountain creeks can stay over smooth stones by using a mechanism consisting of thorns and one sucker [6, 7]. Lizards and geckos can walk over vertical surfaces by exploiting capillary forces combined with a sort of mechanical clamping (with stiff prickles whose dimensions are comparable with the surface rugosity) [8]. Frogs sweat through their fingertips different kinds of biologic glues, so they can stick over slippery surfaces. In addition, they possess peculiar hexagonal cells able to optimize glue delivery [9, 10].

Table 1. Morphological dimensions of *Sobolevitaenia Moldavica* and *Sobolevitaenia Japonensis* parasites.

| | Sobolevit. Moldavica | Sobolevit. Japonensis |
|------------------|---------------------------|---------------------------|
| Rostellum length | 180–207 (μm) | 128–130 (μm) |
| Rostellum width | 84–90 (μm) | 63–75 (μm) |
| Rows number | No. 2 | No. 2 |
| Hooks number | No. 20 | No. 20 |
| First row | 45–47 (μm) | 48–50 (μm) |
| Second row | 40–42 (μm) | 43–45 (μm) |

On the other hand, the gastrointestinal tissue represents a challenging environment for locomotion because it is dynamic (peristalsis contraction), highly corrosive, irregular and slippery. Nevertheless, there are biological systems, like tapeworms, able to survive in such conditions due to their peculiar features (figure 2). *Taenia* possesses a ‘*Scolex*’ (head) with four lateral suckers and a reversible *Rostellum*, equipped with a few rows of hooks. The suckers and the hook rows fix the *Scolex* to the intestinal wall. In such a way the proglottides (body segments of tapeworms) are free to move along the gut lumen.

In figure 3 hook geometries are shown. They have been extracted from literature about two bird parasites, *Sobolevitaenia Moldavica* and *Sobolevitaenia Japonensis* [11, 12]. Main dimensions of these parasites are summarized in table 1.

3. Hook modelling and design

Based on the biological specifications, this section is devoted to identifying the optimal material and fabrication technology for obtaining biomimetic effective hooks.

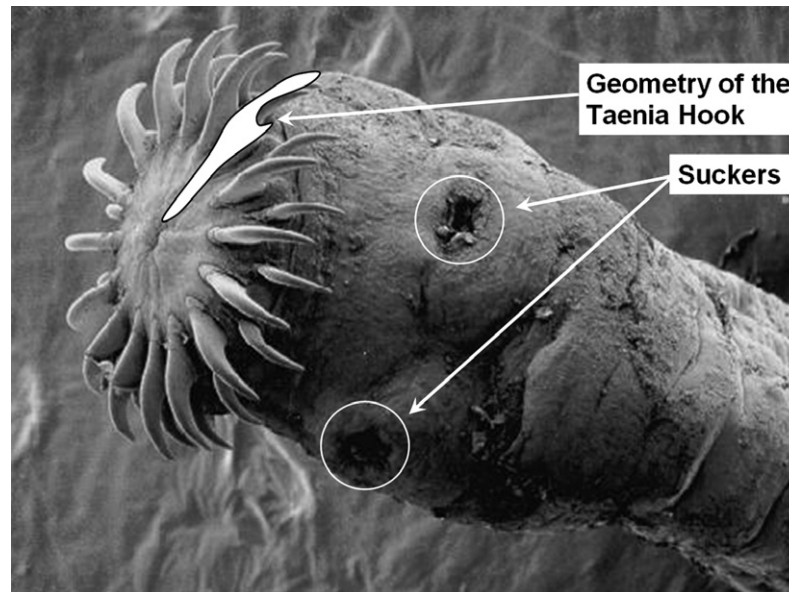


Figure 2. SEM image of the Taenia Solium Scolex.

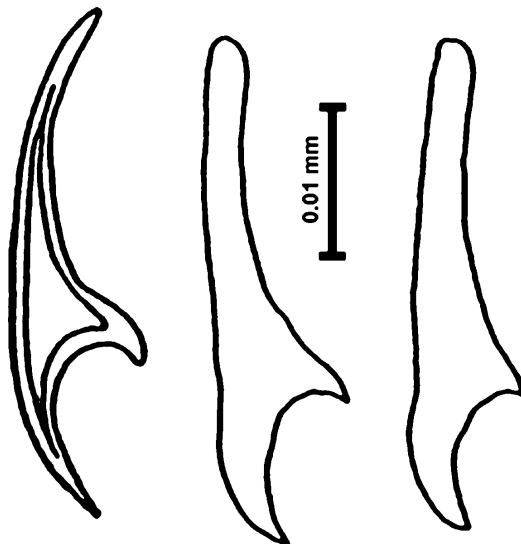


Figure 3. Rostellar hooks shape both present in two bird parasites: Sobolevitaenia Moldavica and Sobolevitaenia Japonensis.

3.1. Selection of the artificial hook material

The material which has been considered for fabricating artificial hooks is *nylon 6*. Such a polymer is normally used for sport fishing monofilaments. It has been selected for our application thanks to the following properties:

- the elastic modulus ($E_{\text{nylon-6}} = 2.85 \text{ Gpa}$) is comparable to hydroxyapatite, that is the principal component of animal bones ($E_{\text{orthophosphate calcium bi hydrate}} \approx 1 \text{ Gpa}$), thus respecting the biomimetic approach of the problem;
- nylon 6 is biocompatible for intestinal application;
- this polymer has good chemical stability against acids;
- the selected polymer is suitable to be melted and then modelled, thanks to its favourable properties in liquid state condition. It has a thermoplastic behaviour, characterized

by a high fluidity of the melted state. A rheological analysis of such material shows tixotropicity (i.e. viscosity decreases by increasing the speed gradient), and a very short relaxation time.

3.2. The 'liquid bridge process': a possible micro-fabrication technology

The shape of a biomimetic hook is very difficult to obtain by using traditional technologies, because it has an unusual geometry and a very small size: it measures about $200 \mu\text{m}$ in length and about $90 \mu\text{m}$ in maximum diameter.

From the literature, it is possible to pick out some interesting processes aimed at fabrication of micro- and nano-needle structures. Very small single-type needles for transdermal drug delivery can be fabricated by means of the reactive ion etching technique [13]. Arrays of silicon micro-tips can be fabricated as well, with different profiles and radii based on specific requests: e.g. for biological applications in the separation process of living cells; for force microscopy, when probe tips are needed; for filter applications in inkjet nozzles, by using the 'black silicon method' [14]. Furthermore, by modifying the black silicon etching technique, it is possible to shape peculiar micro-needles, whose height, base diameter and spacing dimensions are respectively $150 \mu\text{m}$, $50 \mu\text{m}$ and $100 \mu\text{m}$ [15]. These techniques allow us to fabricate very small and reproducible structures, but the obtained micro- and nano-prototypes appear to be not flexible enough for the application proposed in the present paper.

A parallel bio-inspired approach, for fabricating gecko-like nano-hairs, exploits nano-moulding techniques and allows us to obtain nano-structures with 200 nm diameter and $60 \mu\text{m}$ total length [16]. These nano-hairs, although very promising in terms of bio-inspired adhesion capabilities, exploit Van der Waals forces for their proper working, which are completely different forces from those generated by a tapeworm. Moreover, the effectiveness of these

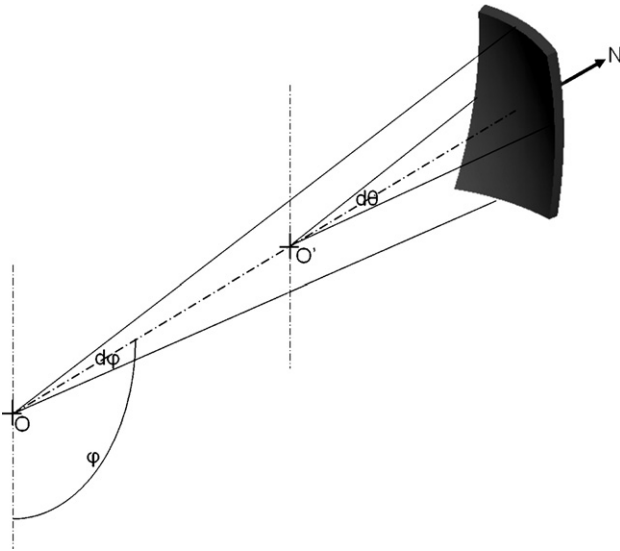


Figure 4. Infinitesimal element of the thin shell.

nano-structures on wet surfaces (i.e. the intestinal wall) must still be proved.

The process proposed in this paper is based on surface tension and capillarity: a drop of polymer is melted between two parallel planes and then stretched by moving the planes apart (a similar method was exploited to fabricate SU-8 nano-fibre structures) [17]. On each plane there is a circular region (of R_{base} radius) wet by nylon 6 liquid, surrounded by a not wettable surface: then a sort of liquid bridge can be shaped. The bases of such bridge are therefore constrained to remain circular (with constant radius) due to the circular wettable surfaces.

A quasi-static motion is achieved thanks to the low speed of the process ($0.05\text{--}5\text{ mm s}^{-1}$), thus cancelling viscous effects and allowing us to neglect mass forces, which are small due to the micro-dimensions of the hooks and due to scaling laws.

Based on the above considerations, the following equation system can be deduced:

- $p = \gamma \left(\frac{\sin \varphi}{r} + \frac{1}{r_1} \right)$: Laplace's equation (equation of equilibrium, obtained by balancing forces along the normal direction of the liquid surface, figure 4) [18],
- $2\pi r \gamma \sin \varphi - p\pi r^2 - F = 0$: axial equilibrium (equation of equilibrium, obtained by balancing forces along the axial direction of the liquid bridge, figure 5),
- $r_1 = -\frac{[1+(r')^2]^{\frac{3}{2}}}{r''}$: geometrical relation (figure 6),
- $\varphi = \arctg(r') + \frac{\pi}{2}$: trigonometrical relation between the involved angles,
- $\int_0^h \pi r(z)^2 dz = \pi R^2 h_0$: volume invariance,

where

- p : relative internal pressure
- γ : surface tension of the melted polymer (at $237\text{ }^\circ\text{C}$)
- $r_1, \frac{\sin \varphi}{r}$: main curvatures
- r : radius of the generic circumference lying over a plane orthogonal to the bridge axis and at a distance ' z ' from the lower reference plane
- F : global axial force generated by the liquid bridge to the support planes (it is assumed positive when it produces an approaching motion of the two parallel planes)

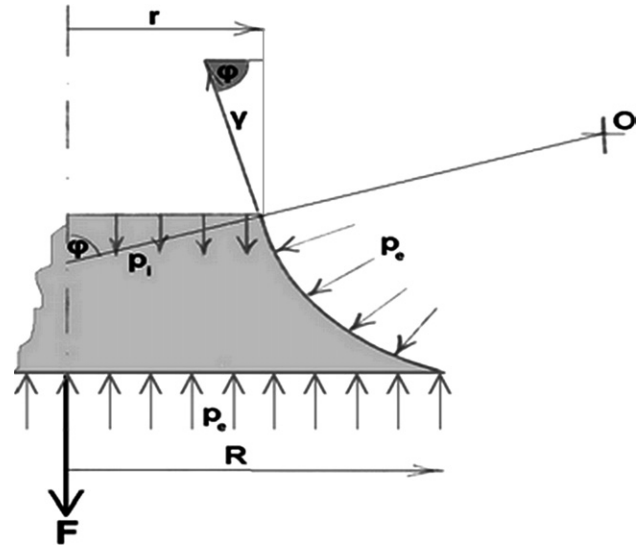


Figure 5. Equilibrium of the forces along the axial coordinate.

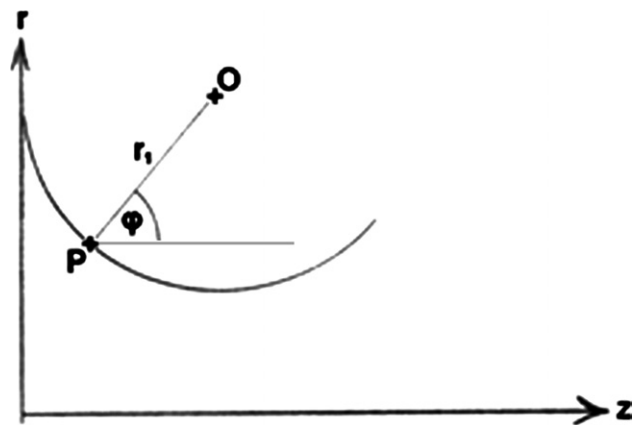


Figure 6. Curvature radius of $y = f(x)$ at the generic point $P(x; y)$.

- r^I, r^{II} : first and second derivatives of the radius with respect to the axial coordinate ' z '
- R : radius of the wettable region over both parallel planes
- h_0 : height of the small polymer cylinder before melting and stretching.

This equation system has five equations and five unknowns (φ, r, r_1, p, F), therefore the problem is well defined. By combining the above equations, a nonlinear, ordinary, second-order differential equation can be obtained:

$$r^{II} = \frac{[1+(r')^2]^{\frac{3}{2}}}{r^2} \left[\frac{F}{\gamma\pi} - \frac{r}{\sqrt{1+(r')^2}} \right].$$

The boundary conditions of the problem are the following:

$$r|_{z=0} = R, \quad r'|_{z=0} = \text{tg} \left(\varphi_A - \frac{\pi}{2} \right)$$

where: φ_A : it is the angle of bridge/substrate contact [19].

The integral equation has been solved by a numerical approach using MatLab[®] software.

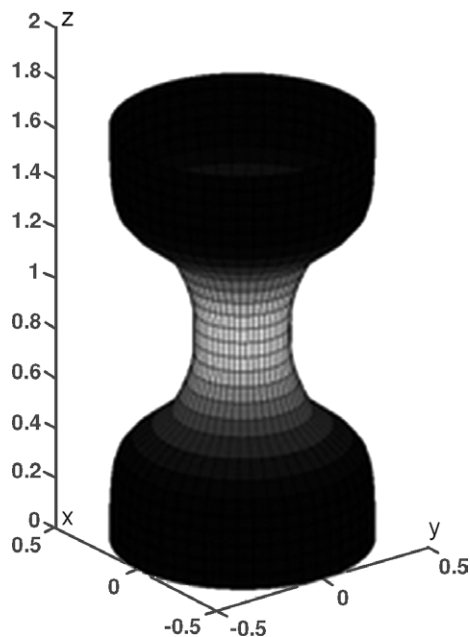


Figure 7. Liquid bridge simulation in MatLab®.

For a given distance between the two parallel planes, the code calculates the bridge geometry and draws its three-dimensional shape (figure 7).

Many simulations have been performed in order to detect the best parameters for obtaining a biomorphic geometry. The conclusion is that the static process enables a hook geometry near to the target shape if large ratios $\frac{h_0}{r}$ are adopted (figure 8).

The quasi-static simulation also shows that the liquid bridge can only produce the main structure of the hook. In

order to fabricate the sharp tip, it is necessary to exploit a different technique, for example a dynamic separation of the two parts, based on a relative movement of the two parallel planes synchronized with a progressive cooling of the throat of the bridge.

4. Experimental setup for hooks fabrication

A dedicated bench has been designed and fabricated to perform fabrication tests, as shown in figure 9. An electrically actuated ring driven by a step motor can slide along a cylindrical chassis guide. Sample temperature is regulated by a closed loop control: a thermocouple measures the temperature, whereas wound coils of known electrical resistance heat the entire chassis by the Joule effect.

Refrigeration is assured by a compressed air circuit, which can freeze the liquid bridge geometry at the desired instant during the test ($T_{\text{glass transition}}^{\text{nylon 6}} = 85^\circ\text{C}$). In particular, external fresh air is conveyed by aspiration through the region where the polymer is stretched. The stroke and the speed of the sliding ring can be controlled by an electronic board to which data are transmitted by a LabView® interface.

The starting material (i.e. segment of nylon wire) is inserted between the two parallel planes (one of the two planes belongs to the chassis, the other one belongs to the sliding ring); thus the temperature of the ring rises to the polymer melting point ($T_{\text{melting}}^{\text{nylon 6}} = 237^\circ\text{C}$), thanks to the heating resistance. Four steps are illustrated in figure 10. In the first one the sample is located between two heated plates and it is still solid; in the second one the polymer melts; in the third one the stretching process is performed, and in the last one the material is cooled down in order to freeze the desired configuration (refer to figures 2 and 3).

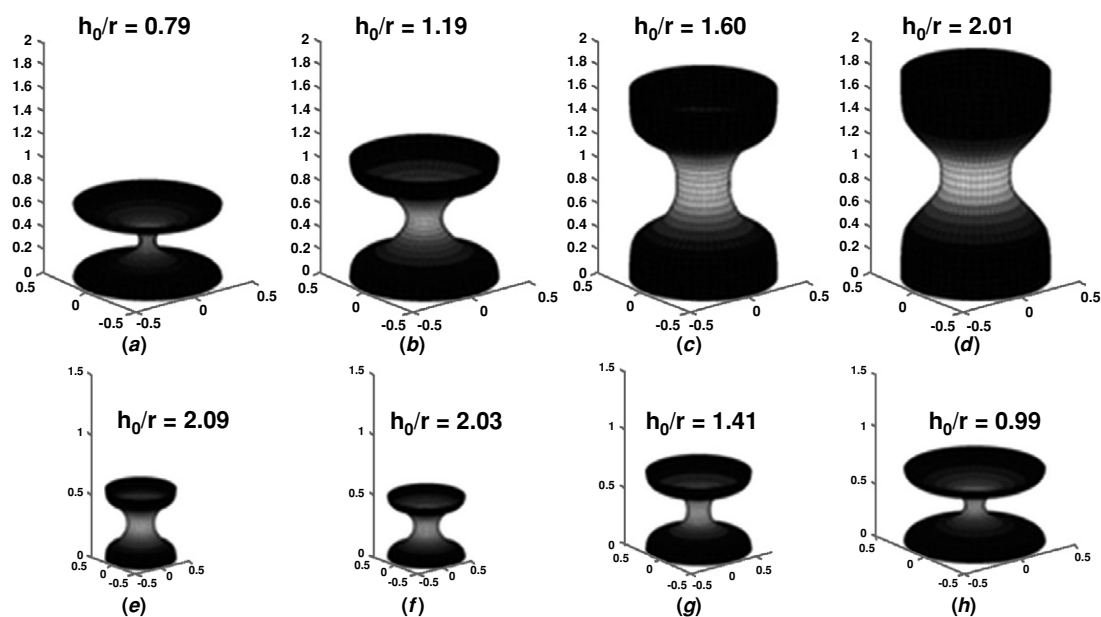


Figure 8. Simulations are obtained for different ratios $\frac{h_0}{r}$; from (a) to (d) base radii remain constant (equal to 0.5 mm) whereas h_0 is equal to 0.39, 0.60, 0.80 and 1.01 mm respectively; from (e) to (h) base radius is equal respectively to 0.23, 0.25, 0.35 and 0.50 mm, whereas h_0 is equal respectively to 0.48, 0.51, 0.49 and 0.50 mm; therefore from (a) to (h) ratio $\frac{h_0}{r}$ is equal respectively to 0.79, 1.19, 1.60, 2.01, 2.09, 2.03, 1.41 and 0.99.

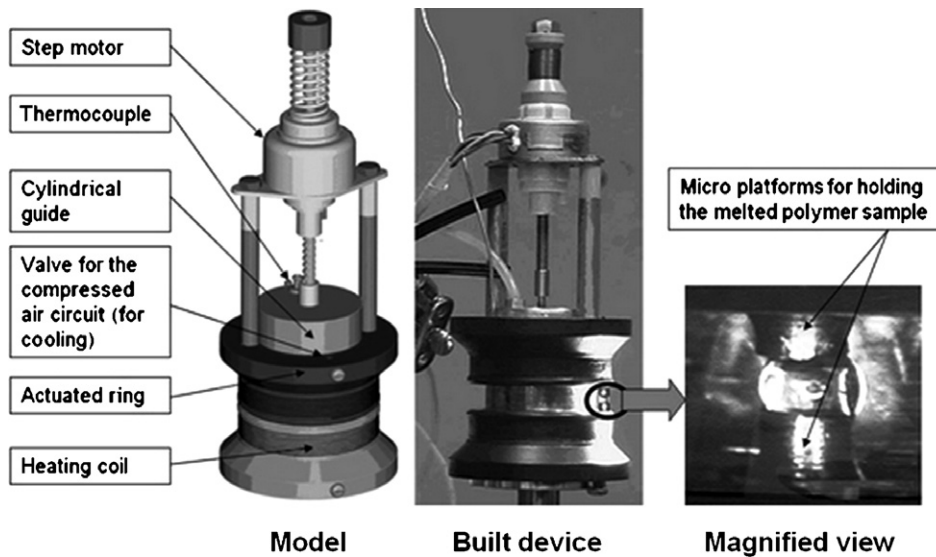


Figure 9. Experimental setup.



Figure 10. Four phases of the liquid bridge formation.

5. Hooks fabrication and performance

Nine typologies of test have been conducted with cylindrical nylon samples having a starting diameter of $100\ \mu\text{m}$ and a height of $130\ \mu\text{m}$. In table 2 experimental data have been summarized by considering motor speed, cooling condition and heating condition.

The goal of the process is to obtain a 'biomorphic hook', which is a 3D geometry with a wide base area and a conic body terminating with a sharp tip.

During the first test, after the polymer melting, the plates were slowly moved apart, without forced cooling. The result was a cylindrical lengthened structure (figure 11). This shape cannot be predicted by quasi-static simulation. In fact, the natural cooling provided by external air to the elongated structure, associated with slow moving motor speed, induced a viscosity increase in the polymer. Viscosity of the liquid allowed the liquid bridge to assume a form that would be impossible in static and Newtonian conditions.

Table 2. Experimental test parameters.

| Test no | Cooling | Heating | Motor speed (mm s^{-1}) | Stroke (mm) |
|---------|------------|------------|---------------------------------------|----------------|
| 1 | None | None | 0.05 | 3.2 |
| 2 | None | None | 2.00 | 2.5 |
| 3 | None | None | 2.00 | >5.0 |
| 4 | Continuous | None | 1.00 | 0.5 |
| 5 | Partial | None | 4.00 | 2.5 |
| 6 | Partial | None | 1.00 | 1.0 |
| 7 | Partial | Continuous | 1.50 | 3.0 |
| 8 | Partial | Continuous | 2.50 | 3.0 |
| 9 | Partial | Continuous | 5.00 | 3.2 |

In the second test the motor speed was increased in order to limit natural cooling occurrence. The final structure showed a less cylindrical shape (figure 12). Therefore, during the third test, the same parameters were applied, and the stretching continued until separation in two parts of the filament. The

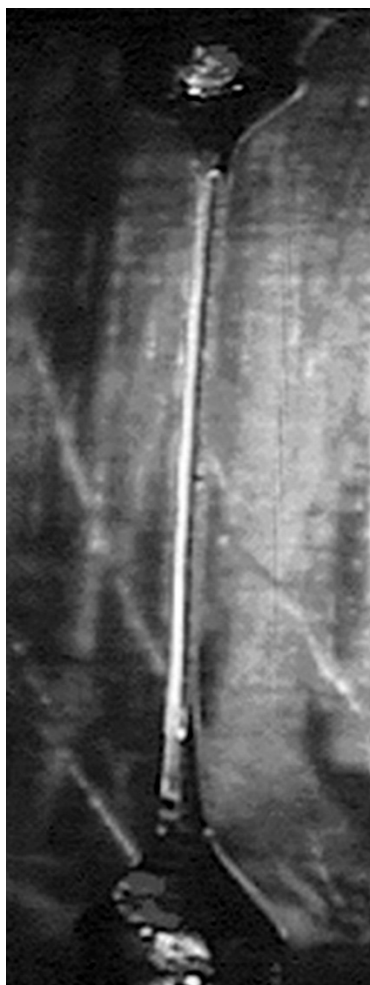
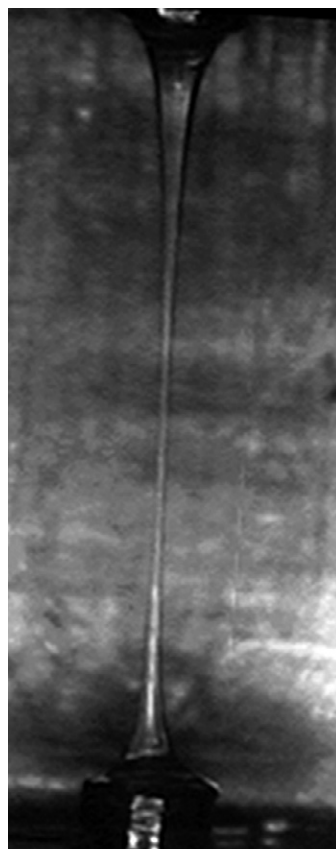


Figure 11. First test result.

obtained structure was very similar to the target geometry, but soon after the separation, the filaments melted again because of the high temperature of the liquid polymer in contact with the warm metal supports.



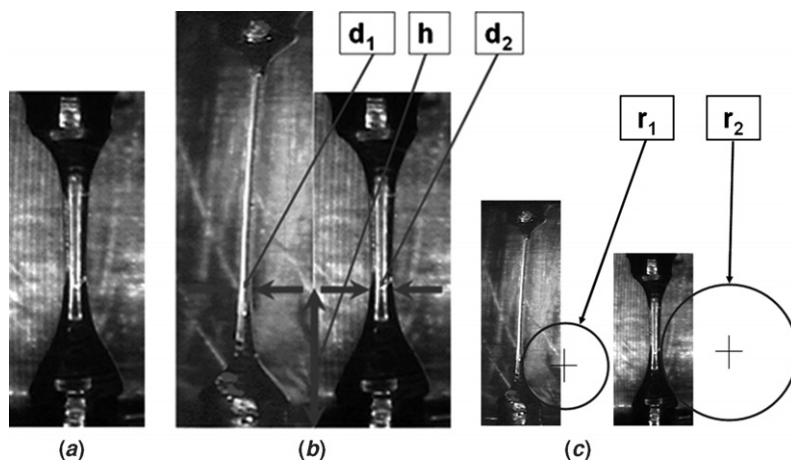
(a)



(b)

Figure 13. (a) Third and (b) fourth test results.

Then a forced cooling was introduced during the fourth test, in order to freeze uniformly the polymeric bridge (not only its thinnest section). The result was an excessive cooling and a loss of the liquid properties before the desired geometry was achieved (figure 13). A partialization of the forced cooling (applied only during the final part of the process) and a speed increase were applied in the fifth test in order to limit this problem.



(a)

(b)

(c)

Figure 12. (a) Second test result; (b) comparison between the first and the second tests: in the first test the shape is longer. In fact the diameter of the second bridge is larger than the first one at the same height h ($d_1 < d_2$); (c) the curvature radius (at the base) of the first bridge is smaller than the second one ($r_1 < r_2$).

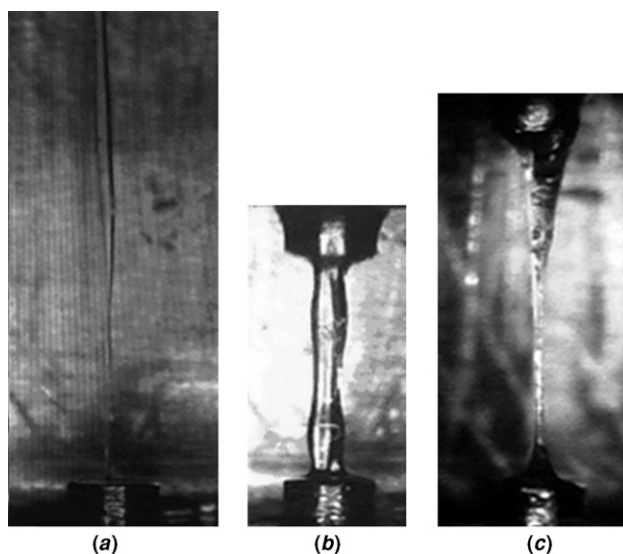


Figure 14. (a) Fifth, (b) sixth and (c) seventh test results.

During the sixth test a shorter stroke was imposed in order to not immediately reach the bridge breaking. The natural process of relaxation, caused by the superficial forces, was stopped before bridge breaking thanks to the forced cooling. The result was an unacceptable and not very controllable process.

In the following tests a further heating was supplied during the stretching phase in order to avoid natural cooling and to control more precisely the bridge geometry by using the forced cooling. In this way larger strokes have been applied without incurring early freezing of the thinnest part of the liquid bridge. In particular, in the seventh test a continuous heating allowed us to obtain a more biomimetic shape while a forced cooling froze such geometry (figure 14).

Also for tests 8 and 9 the same parameters of cooling and heating were used, but operating speed was changed in each test. In particular, in test 9 the best parameters to fabricate a tapeworm-like polymeric hook (figure 15) have been found. The profile is not straight, but slightly bent (as the biological model): this behaviour is due to the weak current of aspirated air, which provokes a lateral force able to shift the bridge striction from the central position of equilibrium.

An array of 16 micro-hooks was fabricated by exploiting the ‘liquid bridge’ technology and by using the cooling and heating parameters of test 9 (figures 16(a) and (b)). Several adhesion experiments were then performed on a strip of gastrointestinal tissue from a pig’s colon *in vitro* (figure 16(c)) and over a piece of wet leather (figure 16(d)). By pulling the array connected to a load cell, the tests demonstrated that each hook is able to generate a maximum adhesion force of 0.19 N on the gastrointestinal tissue and of 0.12 N on the wet leather. Additional dynamic tests proved that each hook, dragged over the substrate at a speed equal to 5.8 mm s^{-1} , is able to generate a resistant force of 0.06 N onto the gastrointestinal tissue and of 0.06 N onto the wet leather. No visible damage occurred over the substrates after the sliding of the hooked device.

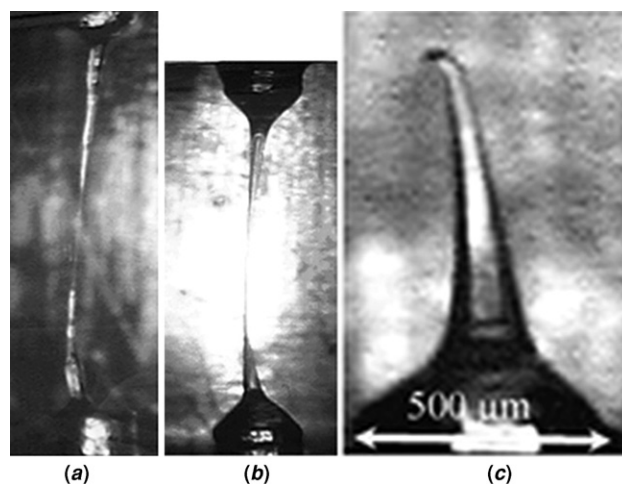


Figure 15. (a) Eighth and (b) ninth test results. Finally (c) the single biomimetic hook after separation.

6. Discussion on the fabrication process

In conditions of high temperature (i.e. minimum viscosity) and low velocity (i.e. quasi-static conditions) the bridge shape matches simulation results, as shown, for example, by comparing figure 7 with the initial shape of the liquid bridge visible in figure 10. When viscosity is increased by cooling, the hottest parts of the liquid bridge, nearest to the substrates, are the only ones identical to the simulation results, as demonstrated in figure 17. These areas—close to the two substrates—can also be considered quasi-static in dynamic conditions, thanks to the adhesion boundary condition always acting even if the substrates are moving with large velocities. In summary, experimental tests proved the validity of the theoretical study if the preliminary hypotheses of the mathematical model are verified, i.e. low viscosity of melted polymer and quasi-static conditions.

The theoretical study is necessary to know the correct ratio $\frac{h_0}{r}$, and thus the initial volume of the sample to be melted, required to obtain a bio-inspired shape of the hook. In fact, the shape of a real tapeworm’s hook can be mainly defined by three geometrical factors: length, base radius and base round. Length depends on the total stroke of the planes moving apart, base radius is imposed by the area of the support where adhesion is constrained, while for the third factor it is enough to impose a given ratio $\frac{h_0}{r}$ and to use the prediction capability shown by the theoretical model. In addition, the theoretical study demonstrates that a dynamic separation is needed, because a quasi-static process does not allow us to obtain a sharp tip—which is typical of tapeworms, but only to shape a biomimetic profile close to the bases.

Practically, performed tests demonstrated that it is possible to achieve a shape of the hook similar to the natural one as shown in figure 3. They also allowed us to understand that it is necessary to carry out some intermediate operations, in order to obtain such biomorphic geometry:

- the initial radius of the sample has to be equal to the base radius of the natural tapeworm hook;
- the initial height of the sample has to be chosen in order to replicate natural tapeworm hook volume;

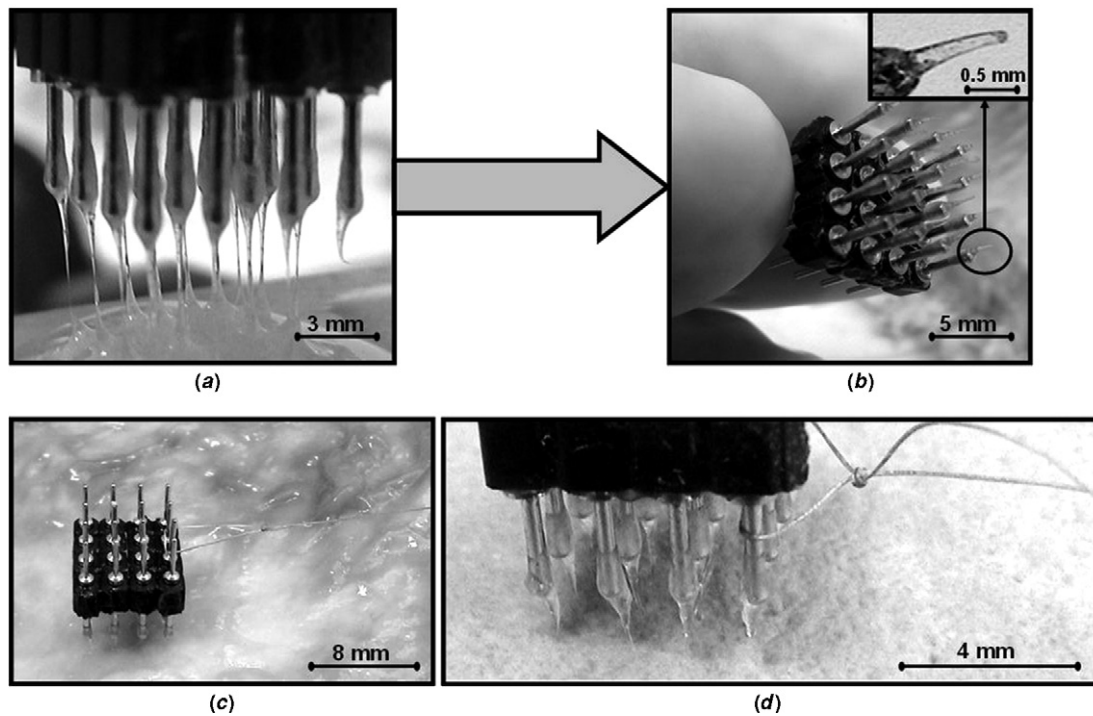


Figure 16. (a) Fabrication of the 16 micro-hook array (b) by means of the ‘liquid bridge’ technology. Adhesion experiments on a strip of gastrointestinal tissue of pig’s colon (c) and on a piece of wet leather (d).

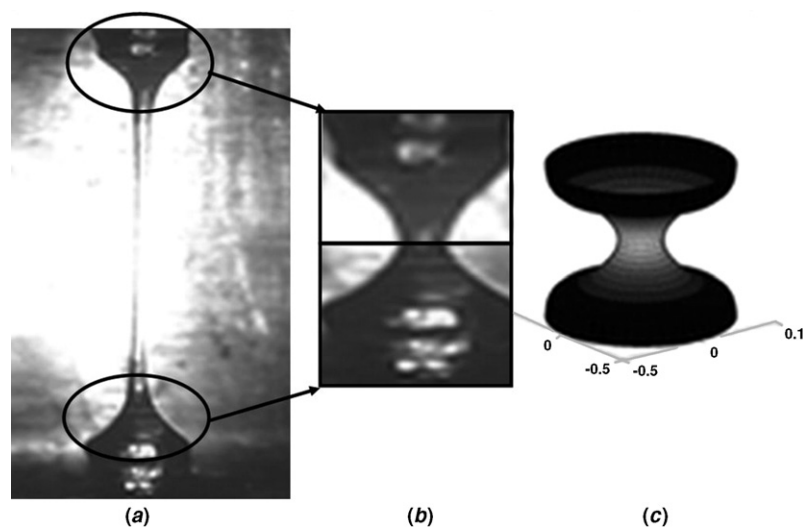


Figure 17. (a) Liquid bridge formation with $\frac{h_0}{r} = 1.3$; (b) and (c) matching between liquid bridge near the basis and simulation result the same ratio.

- the two planes have to be moved apart up to two times the height of the natural parasite hook, because the liquid bridge process allows us to obtain two hooks at the same time;
- once the melting temperature is reached, the polymer has to be maintained in the liquid state by providing the amount of heat which is lost through the entire structure due to convection towards the surrounding air;
- the liquid bridge has to be stretched at the velocity of about 5 mm s^{-1} : such velocity, relatively high, allows us to facilitate the melted polymer stretching due to its intrinsic thixotropy and to reduce the time required by the surrounding air to diffuse around the structure, therefore avoiding cooling and polymer freezing;
- a single stroke must be performed, in order to avoid polymer relaxation. In fact, if two or more strokes are performed, during the time interval between two consecutive strokes the cross polymeric links, which are broken during stretching, have enough time to reshape. As a matter of fact, any viscous flow of melted polymer implies a partial splitting up of cross links in molecular chains. Anyhow the Brownian motions reconstitute completely intermolecular links after a short relaxation time τ ($< 1 \text{ ms}$);

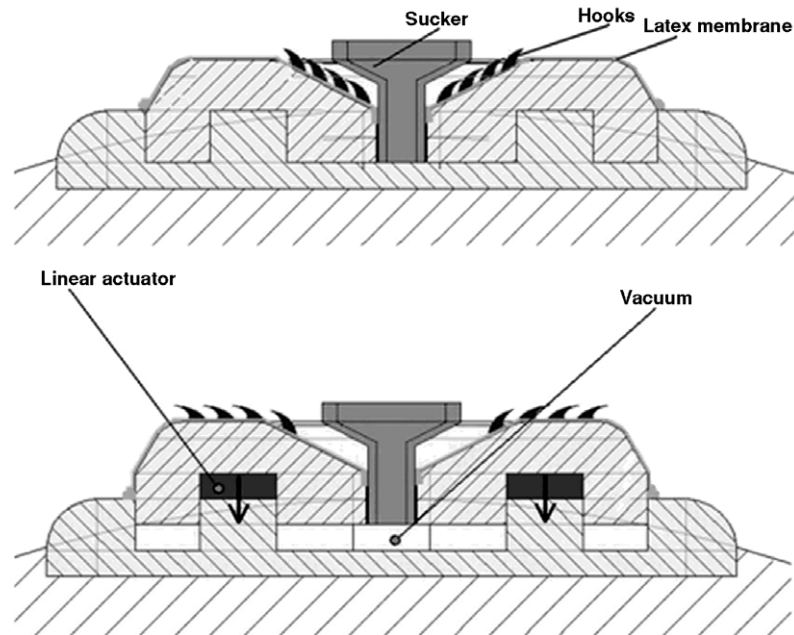


Figure 18. Scheme of functioning of the tapeworm-like device.

- once the required height is reached, it is necessary to check the minimum diameter of the liquid bridge (which is inclined to decrease) until it becomes narrow enough to look like a natural tapeworm hook (refer to figures 2 and 3);
- it is necessary to freeze the achieved shape, by using a stream of fresh air from outside and by interrupting the heating by resistance coils; once frozen (below the transition interval, $T < 85\text{ }^{\circ}\text{C}$), the structure can easily be broken by exerting a traction force of very small magnitude. In fact the very narrow throat opposes a negligible strength: then it can be excluded that breaking occurs in a place different from the throat itself.

7. Hook integration in a polymeric membrane

In this section, future work is presented regarding the development of an integrated system mimicking the whole tapeworm adhesion mechanism [20], including suction and mechanical hooking (figure 18), which is based on the micro-hooks that have been described above.

The whole device consists of a mobile frame, a latex membrane, biomimetic polymeric hooks and a central sucker (fixed to the frame). The frame and the sucker can move thanks to a linear actuation. The latex membrane has a hollow circular shape, where the internal edge is glued to the sucker and the external one is fixed to the frame.

When the bottom frame moves up, a vacuum is generated at the sucker by using a traditional piston system; consequently, the stretching of the elastic membrane makes the hooks protrude. In this way, one actuated degree of freedom produces the vacuum and generates the protrusion of the hooks. This feature could be very useful in terms of integration, power saving and miniaturization, as in the case of endoscopic applications [21].

7.1. Batch fabrication of the biomimetic hooks

Thanks to the previous study on optimal parameters (size of nylon samples, temperature, velocity, etc), instead of fabricating one tip singularly, the liquid bridge process could be implemented for batch production with the unquestionable benefits of a shorter required time and identical hook shape.

A way to reach such a target is to use two metal plates, each one with a matrix of holes. Ducts on the superior plate allow the pressured melted nylon 6 (which is contained in a heated adjacent tank) to enter into the plate holes. Before casting, it is convenient to overspread the cavity walls with detachment agent, in order to facilitate the subsequent removal of the hooks.

The whole process could be divided into two different phases:

- a first static phase;
- a second dynamic phase.

7.2. Static phase

First, the two parallel plates are approached and then heated at the melting point of nylon 6 ($T_{\text{melting}}^{\text{nylon } 6} = 237\text{ }^{\circ}\text{C}$). Then the liquid polymer is injected from the adjacent pressurized camera and the plate cavities are completely filled.

At the bottom of every hole in the lower plate, a small hole ensures there are no air bubbles. The two plates are moved apart at the velocity of 5 mm s^{-1} (figure 19). The final distance ($500\text{ }\mu\text{m}$) allows us to achieve a stable liquid bridge configuration with the minimum striction diameter. According to the theoretical model, it can be calculated once the initial volume and base radius have been derived from the biologic model.

Polymer bridges are then refrigerated at $180\text{ }^{\circ}\text{C}$ in order to stabilize the obtained shapes. With such temperature, viscosity of the polymer increases, without leaving transition interval ($T_{\text{glass transition}}^{\text{nylon } 6} = 85\text{ }^{\circ}\text{C}$).

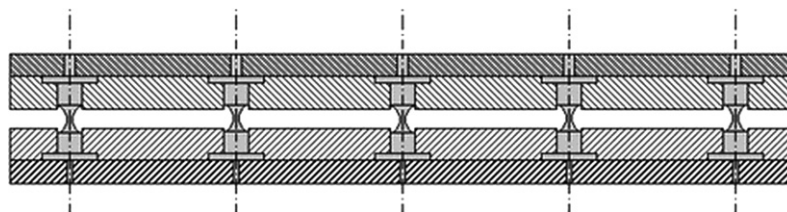


Figure 19. Scheme of the liquid bridge stretching during the static process.

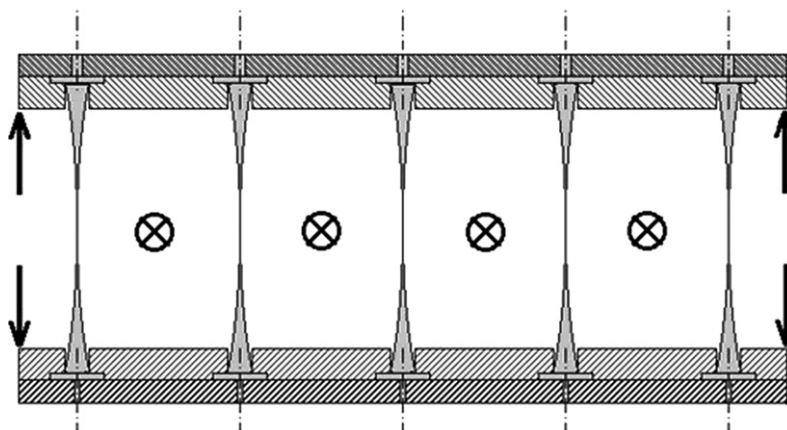


Figure 20. Scheme of the semi-liquid bridge stretching during the dynamic process.

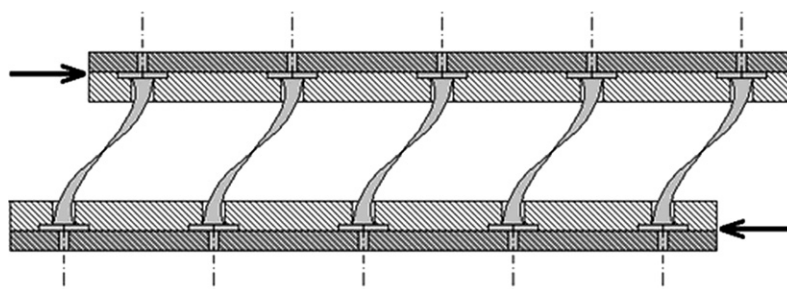


Figure 21. The casting planes slide in opposite directions in order to bend hook axes.

7.3. Dynamic phase

After having shaped the main part of the hook, the biomimetic sharp profile can be obtained through a dynamic phase, consisting of a combination of temperature change, velocity and direction. In addition a further sliding mechanism is required, in order to induce the bending which, in the previous test, is simply provoked by the current of forced cooling air.

At the beginning of the dynamic phase the semi-liquid bridges have to be stretched (figure 20) with a large velocity (about 50 mm s^{-1}). The intrinsic thixotropy of the liquid polymer facilitates such operation: in fact such a property makes the fluid less viscous when subjected to shearing forces and return to the original viscosity in static conditions.

The obtained structure is then cooled down to $180 \text{ }^\circ\text{C}$ in order to increase viscosity but remaining inside the transition interval. The plates have to be slid parallel in opposite directions: in such a way the biomimetic bend can be shaped (figure 21). Finally the tips are cooled under glass transition temperature and then divided, thanks to the very narrow section of the tip as discussed.

8. Conclusions

This paper investigated the possibility of developing a dedicated technique for fabricating biomimetic micro-hooks of nylon starting from the liquid state of the polymer. When a drop of melted polymer is deposited between two heated planes, a sort of liquid bridge is shaped. Based on simulation studies, if the substrates are moved apart with specific stroke and speed, the geometry of a natural *Taenia* hook can be reproduced. An analysis of the surface tension and capillarity effects has been carried out in order to obtain a valid theoretical model explaining the behaviour of the polymer during heating and cooling processes. A numerical simulation of the 'liquid bridge process' has been performed by using MatLab[®] software.

The experimental results of polymer micro-structures match the mathematical previsions. The shape of the artificial hooks accurately imitates the biological model. Figure 22 illustrates the shape of an artificial hook fabricated by the proposed liquid bridge technology, compared with the shape of a natural hook, on the same scale. In addition to the similar shape, the material utilized for fabricating the artificial

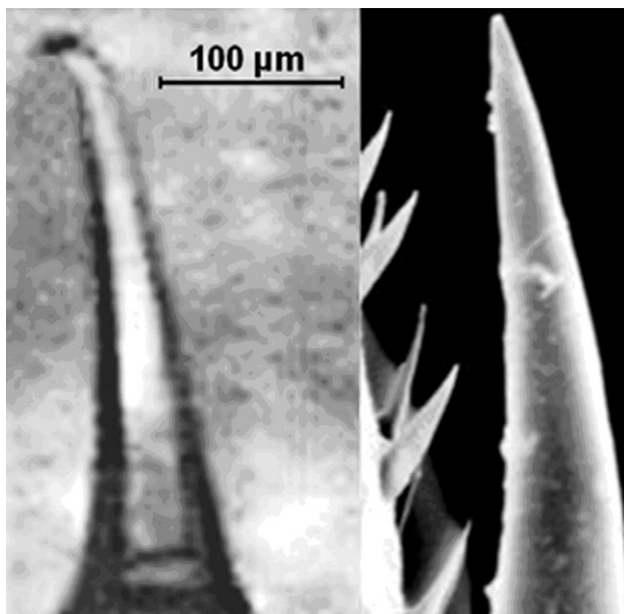


Figure 22. Comparison between artificial hook (on the left) and natural tapeworm hook (on the right).

hook is nylon 6, a polymer whose constitutive behaviour is very similar to hydroxyapatite, the calcium compound that composes animal bones. Nylon 6 chemical composition is $(-\text{CO}-(\text{CH}_2)_5-\text{NH}-)_m$; thus it is composed of C, O, H and N elements, the principal constituents of biological materials.

Consequently, analogies between artificial hooks and biological hooks are in terms of:

- geometry (figure 22);
- working principle (i.e. biomimetic hooking);
- material.

These analogies also allow us to predict a similarity between the effect of the parasite clamping mechanism and the effect of the artificial nylon hook when interacting with the gastrointestinal tissue.

Acknowledgments

The activity presented in this paper has been carried on with the support of the European Commission, in the framework of the BIOLOCH Project (BIOmimetic structures for LOComotion in the Human body—IST FET Programme, IST-2001-34181). The authors wish to thank Mr Carlo Filippeschi and Mr Gabriele Favati for their technical help.

References

- [1] http://www.cancer.org/docroot/STT/stt_0.asp, 16/05/2005
 [2] Gorb S N 1998 Friction systems of insects *Technical Biology and Bionics* (Original title: Reibungssysteme bei Insekten.

In Technische Biologie und Bionik) (Munich: Bionik-Kongress) pp 185–9

- [3] Phee L, Accoto D, Menciassi A, Stefanini C, Carrozza M C and Dario P 2002 Analysis and development of locomotion devices for the gastrointestinal tract *IEEE Trans. Biomed. Eng.* **49** 613–6
 [4] Irschick D J, Vanhooydonck B, Herrel A and Andronescu A 2003 Effects of loading and size on maximum power output and gait characteristics in geckos *J. Exp. Biol.* **206** 3923–34
 [5] Scherge M and Gorb S 2000 *Biological Micro- and Nano-Tribology—Nature's Solutions* (Berlin: Springer) pp 95–96, 98–100, 114–116, 119–121
 [6] Singh N and Agarwal N K 1993 Organs of adhesion in four hillstream fishes: a comparative morphological study *Advances in Limnology* (New Delhi: Narendra) pp 311–6
 [7] Singh N and Agarwal N K 1991 The SEM surface structure of the adhesive organ of *Pseudoecheneis sulcatus* McClelland from Garhwal Himalayan hillstreams *Acta Ichthyologica Piscatoria* **21** 29–35
 [8] Autumn K, Liang Y A, Hsieh S T, Zesch W, Chan W P, Kenny T W, Fearing R and Full R J 2000 Adhesive force of a single gecko foot-hair *Nature* **405** 681–5
 [9] Hanna G and Barnes W J P 1991 Adhesion and detachment of the toe pads of tree frogs *J. Exp. Biol.* **155** 103–25
 [10] Nachtigall W 1974 *Biological Mechanisms of Attachments: the Comparative Morphology and Bioengineering of Organs for Linkage, Suction, and Adhesion* (New York: Springer)
 [11] Kugi G 2000 *Sobolevitaenia japonensis* n. sp. (Dilepididae: Dilepidinae) from a dusky thrush, *Turdus naumanni* eunomus Temminck *Parasitol. Int.* **48** 199–203
 [12] Kugi G and Fujino T 1999 A new avian cestode *Malika turdi* n. spp. (Dilepididae: Dipylidiinae) from the golden mountain thrush, *Turdus dauma aureus* Holandre *Parasitol. Int.* **48** 179–82
 [13] Henry S, McAllister D V, Allen M G and Prausnitz M R 1998 Microfabricated microneedles: a novel approach to transdermal drug delivery *J. Pharm. Sci.* **87** 922–5
 [14] Jansen H, de Boer M, Otter B and Elwenspoek M 1995 Black silicon method: IV. The fabrication of three-dimensional structures in silicon with high aspect ratios for scanning probe microscopy and other applications *Proc. IEEE Micro Electro Mechanical Systems Conf.* pp 88–93
 [15] Prausnitz M R, McAllister D V, Kaushik S, Patel P N, Mayberry J L and Allen M G 1999 Microfabricated microneedles for transdermal drug delivery *Bioeng. Conf. (Big Sky, MT)*
 [16] Sitti M and Fearing R S 2003 Synthetic gecko foot-hair micro/nano-structures as dry adhesives for future wall-climbing robots *J. Adhes. Sci. Technol.* **17** 1055–73
 [17] Nain A S and Sitti M 2003 3-D nano-fiber manufacturing by controlled pulling of liquid polymers using nano-probes *IEEE-NANO* pp 60–3
 [18] Timoshenko S P and Goodier J N 1987 *Theory of Elasticity* 3rd edn (New York: McGraw-Hill)
 [19] Knapp H F and Stemmer A 1999 Preparation, comparison, and performance of hydrophobic AFM tips *Surf. Interface Anal.* **27** 324–31
 [20] Menciassi A, Stefanini C, La Spina G and Dario P 2002 Bio-inspired solutions for locomotion in the gastrointestinal tract: background and perspectives *EPSRC/BBSRC International Workshop Biologically-Inspired Robotics: The Legacy of W Grey Walter Conference, GWG'02 (Bristol, UK)* pp 182–7
 [21] Iddan G, Meron G, Glukhovskiy A and Swain P 2000 Wireless capsule endoscopy *Nature* **405** 417